NCTS Taiwan-Japan Symposium on Celestial Mechanics and N-Body Dynamics 2013
Proceedings of NCTS Taiwan-Japan Symposium, 2013
Eds. K.C. Chen, M. Saito, M. Sekiguchi and M. Shibayama

Direct N-body Simulations of Aggregate Collisions in the Tidal Environment

Ryuki Hyodo

Department of Earth and Planetary Sciences, Kobe University, Kobe 657-8501, Japan

Abstract. Outcomes of collisions in free space is regulated by specific impact energy, and the mass fraction of the largest remnant is a monotonically decreasing function of impact energy. However, it is not obvious whether such relationship is directly applicable to collision in the tidal environment. In this work, I perform local N-body simulations in order to investigate the collisional disruption of gravitational aggregates in the strong tidal environment corresponding to Saturn's F ring as done by Hyodo & Ohtsuki (2014). Numerical results show different behavior from those in free space and outcomes depend on impact velocity and impact direction. Simulations show that collisions in the azimuthal direction are much more destructive than those in the radial direction, and collisions in the radial direction sensitively depend on the impact velocity. In addition, they show that a complete disruption of aggregates can occur even in impacts with velocity much lower than aggregate's escape velocity. In such low-velocity collisions, the deformation of colliding aggregates plays an essential role in determining final outcomes, because the physical size of the aggregate is comparable to its Hill radius (Hyodo & Ohtsuki 2014).

1. Introduction

Saturn's F ring is located just outside Saturn's Roche limit, and thus the effect of tidal force is not negligible. Cassini spacecraft suggests gravitational accretion of ring particles in the Roche zone (Porco et al. 2007). The effect of the tidal force becomes negligible far outside the Roche limit,

[1]ryukih@stu.kobe-u.ac.jp

and particles with arbitrary mass ratios are able to form gravitational aggregates. On the other hand, in the tidal environment where the effect of tidal force is important, collisions between particles or aggregates lead not only to accretion but also to disruption (Karjalainen 2007). For example, Voyager images show transient brightening events in Saturn's F ring (Showalter 1998), and collisions between embedded bodies have been proposed as the cause of these events (Barbara & Esposito 2002). Recently, Cassini spacecraft observed small protrusions from the core of the F ring, called 'mini-jets', and they are regarded as a result of low-velocity collisions within the ring (Attree et al. 2012). Disruptional processes of planetary bodies have been extensively studied in the contexts of planetary accretion or asteroid dynamics. However, since the effect of the tidal force is not taken into account in these works, we cannot directly apply results of these studies to tidal environment. In the present work, I will investigate aggregate collision in the strong tidal environment corresponding to Saturn's F ring on various impact velocities and impact directions.

2. Numerical methods

In the present work, I perform simulations of aggregate collision using local N-body simulation code that deals with gravitational interactions and inelastic collisions between particles in the Hill coordinate system (Hyodo & Ohtsuki 2014). Motion of two particles i and j in the Hill coordinate system (x, y, z) with the origin moving on a circular orbit at the distance a from the central planet with the Keplerian angular velocity Ω, where the x-axis is pointing radially outward, the y-axis pointing towards the orbital motion, and the z-axis is perpendicular to the x-y plane. Suppose that the mass and position vector of particle i are given by m_i and $\vec{r}_i = (x_i, y_i, z_i)$, respectively. In this case, linearized equations of motion for particle i are described as

$$\begin{aligned} \ddot{x}_i &= 2\Omega\dot{y}_i + 3\Omega^2 x_i + \frac{Gm_j\,(x_j - x_i)}{r_{ij}^3} \\ \ddot{y}_i &= -2\Omega\dot{x}_i \qquad + \frac{Gm_j\,(y_j - y_i)}{r_{ij}^3} \\ \ddot{z}_i &= \qquad -\Omega^2 z_i \;\; + \frac{Gm_j\,(z_j - z_i)}{r_{ij}^3} \end{aligned} \tag{1}$$

where G is the gravitational constant and $r_{ij} \equiv |\vec{r}_i - \vec{r}_j|$. The equations for the relative motion can be written in a form similar to Equation (1) (Nakazawa et al. 1989, Ohtsuki 2012), which we solve to obtain relative

velocities at impact.

Particle trajectories are integrated by using the second order symplectic leapfrog method (Quinn et al. 2010). When collisions between particles are detected, velocity changes are calculated based on the hard-sphere model. I assume that particles are smooth spheres with normal coefficient of restitution, $\varepsilon_{\rm n} = 0.25$.

Figure 1 shows the initial conditions of the impact simulations (Hyodo & Ohtsuki 2014). Two identical aggregates are placed in the Hill coordinate system, so that initially they are just touching each other, either in the radial, azimuthal and vertical direction. Then, an initial velocity of the same magnitude but in the opposite direction is given to each of the aggregates, so that the center of mass of the system is fixed at the origin.

Collision between the two aggregates can result in total accretion, complete disruption, or partial disruption with re-accumulation of some of constituent particles, depending on parameters. At the end of each simulation, I examine the masses of the largest and the second largest remnant aggregates. In order to eliminate the influence of the aggregate shape, I used the same aggregate shape in simulations that is constructed from 500 identical particles with density 0.9 g cm^{-3} and has a certain aspect ratio in simulations.

3. Results

In this section, I present the results of impact simulations of gravitational aggregates in the strong tidal environment corresponding to Saturn's F ring as done by Hyodo & Ohtsuki (2014).

Figure 2 shows the plots of mass fractions of the largest (red squares) and the second largest (blue circles) remnant aggregates at the end of simulation, as a function of impact velocity. In the bottom horizontal axis, impact velocity scaled by the escape velocity is shown, while the upper horizontal axis represents corresponding value of the impact velocity when the radius of the constituent particles is 130 m and their internal density is 0.9 g cm^{-3}. In the case of collision in free space, the mass fraction of the largest remnant decreases as increasing impact velocity (Leinhardt & Stewart 2012). In contrast, numerical results showed that outcomes of collisions in the strong tidal environment show completely different behavior.

The top panel of Figure 2 shows results for radial collisions. It shows complicated dependence of the collision outcome on impact velocity. Figure 3 shows time evolutions of several simulations in this case. When the impact velocity is very small, the colliding aggregates become separated

due to Coriolis force and the Kepler shear after their first contact. As a result, both aggregates remain nearly intact, the mass of each aggregate being kept close to half of the total mass (Region A in the top panel of Figure 2). With slightly higher impact velocity, the area of contact surface of the colliding aggregates at the time of impact becomes significant, and the aggregates apparently form a combined object. However, because the mass of the combined object is not sufficiently concentrated around its center of mass, it gradually becomes elongated due to the tidal force. In this case, part of the aggregate overflows its closed zero-potential surface, leading to total disruption (e.g., the case with $v_{\rm imp}/v_{\rm esc} = 0.69$, which is in Region B in Figure 2, top; see also Figure 3, left). This mode of disruption in the low-velocity regime is a direct consequence of the strong tidal effect, and never happens in the case of collisions in free space, where lower impact velocities prone to be gravitational accretion. With additional slight increase in impact velocity, the mass of the combined object formed immediately after collision becomes sufficiently concentrated around its center of mass. This stabilizes the combined object, resulting in total accretion (e.g., the case with $v_{\rm imp}/v_{\rm esc} = 1.14$, which is in Region C in Figure 2, top; see also Figure 3, middle). When the impact velocity is slightly increased further from the case of Region C, however, collision outcome becomes total disruption again (e.g., the case with $v_{\rm imp}/v_{\rm esc} = 1.52$, which is in Region D in Figure 2, top; see also Figure 3, right). This is because the combined object rotates counter-clockwise around the center of mass after impact due to the Coriolis force. Because of this rotation, the combined aggregate is elongated in the radial direction, resulting in eventual disruption. As seen above, in these cases of relatively low-velocity impacts under the strong tidal force, the shape of the combined aggregate immediately after the impact plays an important role in determining the final collision outcome.

The higher impact velocity somewhat diminishes the rotation effect mentioned above, resulting in almost total accretion (the case with $v_{\rm imp}/v_{\rm esc} = 1.90$). In this case and other cases with still higher impact velocities (i.e., the cases in Region E in Figure 2, top), the mass fraction of the largest remnant is regulated by impact velocity as in the case of collisions in free space, in contrast to the low-velocity regime (Regions A to D) where the aggregate shape after collision regulates the collision outcome. In this high-velocity regime (Region E in Figure 2, top), where the impact energy is large enough, constituent particles in the colliding aggregates can have sufficiently high velocity after impact to escape from the gravity of aggregates, leading to dispersal of the aggregates. As a result, the mass fraction of the largest remnant is a monotonically decreasing function of impact velocity

in this regime.

On the other hand, the middle panel of Figure 2 shows results of simulations of azimuthal collisions in the strong tidal environment. In this case, even with zero or very small impact velocity, the accelerated motion in the azimuthal direction due to mutual gravitational attraction between the colliding aggregates causes the Coriolis force in the radial direction. As a result, the combined aggregate becomes elongated in the radial direction quickly. At the current radial distance from Saturn, the closed zero-potential surface of the aggregate is almost comparable to its physical size. Therefore, this elongation to the radial direction soon results in total disruption. With higher impact velocity, in addition to the effect of tidal elongation of the combined aggregate in the radial direction, some particles have sufficiently high velocity immediately after the impact to escape from the gravity of the combined aggregate, further facilitating disruption.

The bottom panel of Figure 2 shows results of simulations of vertical collisions at the same radial location. numerical results showed that there is a sharp transition between accretion and disruption at $v_{\rm imp}/v_{\rm esc} \simeq 0.5$. As described above, at the radial distance considered here the initial physical size of each aggregate is comparable to its Hill radius. Low-velocity impacts with $v_{\rm imp}/v_{\rm esc} \lesssim 0.5$ result in accretion, because deformation of the combined aggregate is small and all constituent particles settle inside the Hill sphere after the impact. However, when $v_{\rm imp}/v_{\rm esc} \gtrsim 0.5$, the combined aggregate becomes radially elongated after the impact and keeps changing its shape due to the tidal force and the shear motion, and is eventually totally disrupted. With still higher impact velocity, not only the elongation of the aggregate shape but also part of the constituent particles are gravitationally dispersed as a result of collisions facilitates disruption. Therefore, in the strong tidal field corresponding to the F ring, collision outcomes are completely different from those in frees space and among radial, azimuthal, and vertical collisions.

4. Conclusions

In this work, I conducted impact simulations of gravitational aggregates in the strong tidal environment corresponding to Saturn's F ring by using local N-body simulations (Hyodo & Ohtsuki 2014). Mass fraction of the largest remnant after the collision in the free space is monotonically decreasing function of impact velocity. However, numerical results showed that outcomes of aggregate collision in the strong tidal environment largely depend on impact direction (radial, azimuthal and vertical) and show dif-

ferent dependences on impact velocity. Collision in the azimuthal direction is the most destructive, while a radial collision is the least destructive. In the case of radial collisions, collision outcomes are sensitive to impact velocity. Tidal deformation of aggregates after the collision plays an essential role in low-velocity collisions and even much smaller impact velocities than aggregate's escape velocity lead to total disruption. More details and dependences of collision outcomes on other parameters, such as initial aggregate shape, radial distance from the central planet and coefficient of restitution are discussed in Hyodo & Ohtsuki (2014).

5. Acknowledgments

I thank all participants to 2013 NCTS Taiwan-Japan Symposium on Celestial Mechanics and N-Body Dynamics for useful discussions.

References

Attree, N. O., Murray, C. D., Cooper, N. J., & Williams, G. A. 2012, ApJL, 755, L27

Barbara, J. M., & Esposito, L. W. 2002, Icar, 160, 161

Hyodo, R. & Ohtsuki, K., 2014, ApJ, 787, 56

Karjalainen, R. 2007, Icar, 189, 523

Leinhardt, Z. M., & Stewart, S. T. 2012, ApJ, 745, 79

Nakazawa, K., Ida, S., & Nakagawa, Y. 1989, A&A, 220, 293

Ohtsuki, K. 2012, PThPS, 195, 29

Porco, C. C., Thomas, P. C., Weiss, J. W., & Richardson, D. C. 2007, Sci, 318, 602

Quinn, T., Perrine, R. P., Richardson, D. C., & Barnes, R. 2010, AJ, 139, 803

Showalter, M. R. 1998, Sci, 282, 1099

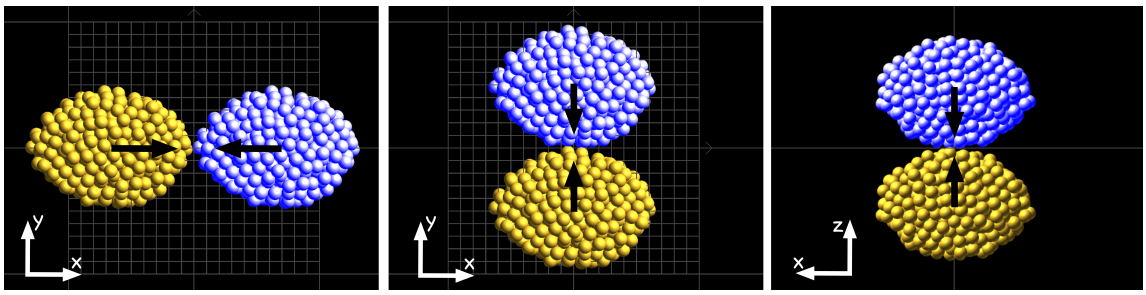

Figure 1. Initial condition of the impact simulation. Aggregates are initially touching each other. The left, middle and right panel shows collision in the radial, azimuthal and vertical direction, respectively in the Hill coordinate. In the left and middle panels Saturn is to the left, and orbital motion is upward. In the right panel, Saturn is to the right. The black arrows show the directions of initial velocities of each aggregate. Taken from Hyodo & Ohtsuki (2014).

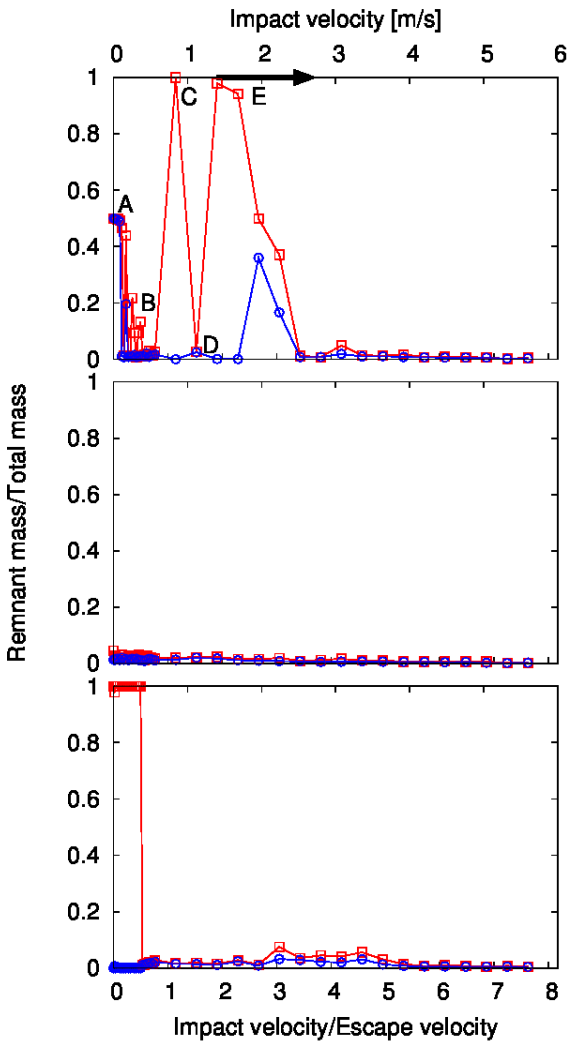

Figure 2. Mass fractions of the largest (red squares) and the second largest (blue circles) remnant obtained at the end of simulations, as a function of impact velocity in the case of a strong tidal environment corresponding to the location of Saturn's F ring (a = 140,000 km). Top, middle, and bottom panels show the results of collision in the radial, azimuthal, and vertical direction, respectively. The vertical and horizontal axes represent the mass fraction scaled by the total mass of the colliding aggregates, and impact velocity $v_{\rm imp}$ scaled by the escape velocity $v_{\rm esc}$ of a spherical body that has the mass of the initial aggregate with particle density of 0.9 g cm^{-3}, respectively. Upper horizontal axis represents corresponding value of the impact velocity when the radius of the constituent particles is 130 m and their internal density is 0.9 g cm^{-3}. Taken from Hyodo & Ohtsuki (2014).

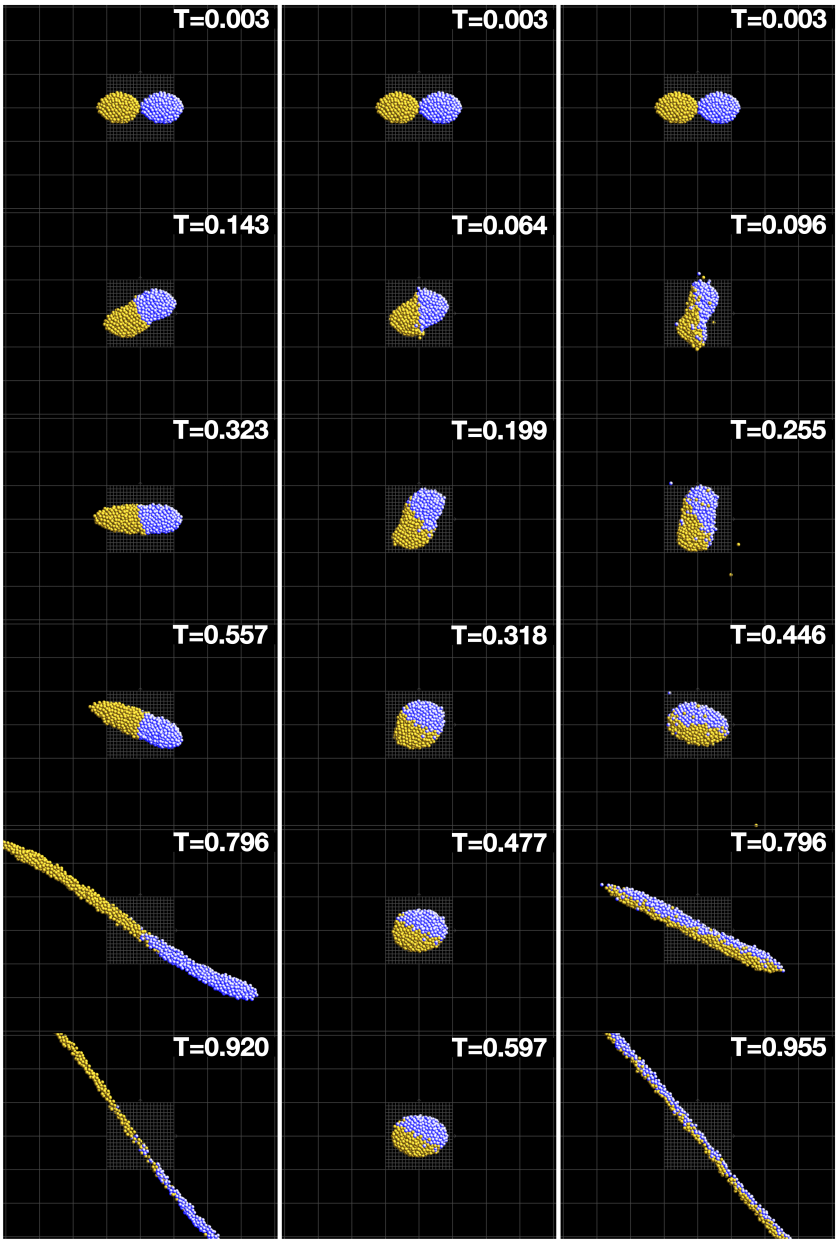

Figure 3. Time series of simulations of collisions between aggregates in the radial direction in the strong tidal environment corresponding to the location of Saturn's F ring (a = 140,000 km). Saturn is to the left and orbital motion is upward. Three cases of relatively low-velocity impacts are shown. Left: total disruption ($v_{\rm imp}/v_{\rm esc}$ = 0.69, Region B in Figure 2, top). Middle: total accretion ($v_{\rm imp}/v_{\rm esc}$ = 1.14, Region C in Figure 2, top). Right: total disruption ($v_{\rm imp}/v_{\rm esc}$ = 1.52, Region D in Figure 2, top). Numbers in each panel represent the time elapsed since the start of simulation in units of the orbital period at the radial location of the origin of the system. Taken from Hyodo & Ohtsuki (2014).